CRISPR TECHNOLOGY

MIC-Drop: A platform for large-scale in vivo CRISPR screens

Saba Parvez[1], Chelsea Herdman[2], Manu Beerens[3], Korak Chakraborti[1], Zachary P. Harmer[1]†, Jing-Ruey J. Yeh[4], Calum A. MacRae[3], H. Joseph Yost[2], Randall T. Peterson[1]*

CRISPR-Cas9 can be scaled up for large-scale screens in cultured cells, but CRISPR screens in animals have been challenging because generating, validating, and keeping track of large numbers of mutant animals is prohibitive. Here, we introduce Multiplexed Intermixed CRISPR Droplets (MIC-Drop), a platform combining droplet microfluidics, single-needle en masse CRISPR ribonucleoprotein injections, and DNA barcoding to enable large-scale functional genetic screens in zebrafish. The platform can efficiently identify genes responsible for morphological or behavioral phenotypes. In one application, we showed that MIC-Drop could identify small-molecule targets. Furthermore, in a MIC-Drop screen of 188 poorly characterized genes, we discovered several genes important for cardiac development and function. With the potential to scale to thousands of genes, MIC-Drop enables genome-scale reverse genetic screens in model organisms.

Historically, large-scale genetic screens in zebrafish have used forward genetic techniques such as chemical or insertional mutagenesis (fig. S1A) (*1*, *2*). These screens have proven invaluable in identifying key pathways regulating vertebrate development (*3*–*5*) and behavior (*6*, *7*). Although impressive in scale, forward genetic techniques are time and labor intensive, requiring years to link a desired phenotype with the genotype. Reverse genetics approaches such as CRISPR have the potential to circumvent some of the issues of forward genetics but are severely limited in throughput (*8*, *9*). Targeting genes of interest is typically done one gene at a time, designing individual guide RNAs (gRNA), injecting Cas9-gRNA ribonucleoprotein (RNP) complexes, and maintaining, propagating, and genotyping groups of fish, all of which require extensive time, labor, and space. The largest such screen to date targeted 128 genes in zebrafish (*10*, *11*). Recent studies using multiplexed gRNAs to generate biallelic F_0 mutants that successfully phenocopy germline mutant phenotypes are a welcome step but have not been scaled up for genome-wide CRISPR screens (*10*, *12*–*17*).

We have developed a platform, Multiplexed Intermixed CRISPR Droplets (MIC-Drop), for performing large-scale reverse genetic screens in zebrafish (Fig. 1A). The platform uses microfluidics to generate nanoliter-sized droplets, each containing Cas9, multiplexed gRNAs targeting a gene of interest, and a unique barcode associated with each target gene. Droplets targeting hundreds to thousands of different genes are intermixed together and injected into zebrafish embryos from a single needle (movie S1). Embryos are raised en masse, and then those exhibiting the phenotype(s) of interest are isolated and the identities of the perturbed genes are rapidly uncovered by retrieving and sequencing the barcodes. The ability to inject all intermixed droplets from a single needle circumvents the laborious and wasteful process of filling a separate needle for each gene targeted. The ability to identify perturbed genes by retrieving barcodes circumvents the need to raise each injected animal separately or deconvolute the mutated gene through genome sequencing.

After testing different surfactant-oil combinations, we identified a particular combination of fluorinated oil and a fluorosurfactant as optimal for droplet generation using a repurposed Bio-Rad QX-200 droplet generator (for more details, see the supplementary text and materials and methods). The droplets generated were uniform and ~100 μm in diameter (Fig. 1B). Each droplet contained four gRNAs targeting a gene of interest. We found that using four gRNAs per gene recapitulated the phenotypes of homozygous mutants in F_0 embryos with high penetrance (fig. S1, B to D, and table S1). Injection of four gRNAs targeting *tyr*, *tnnt2a*, *tbx5a*, *rx3*, *npas4l*, *chrd*, *tbx16*, and *fgf24* resulted in highly efficient biallelic mutagenesis (fig. S2, A and B) and the expected *sandy* (lack of pigmentation), *silent heart*, *heartstrings*, *eyes missing*, *cloche*, *chordino* (tissue ventralization), *spadetail*, and *ikarus* (lack of pectoral fins) mutant phenotypes, respectively, in 70 to 100% of the F_0 embryos. No substantial toxicity was observed in embryos injected with MIC-Drop except for the low level of nonspecific morphological defects typical of traditional RNP injection (Fig. 1, C and D, and figs. S1E and S3, A and B). Droplets were stable during prolonged storage and showed high phenotypic penetrance even after a month of storage at 4°C (Fig. 1D). Additionally, after generating and injecting a mini-library of MIC-Drops, with each droplet targeting any one of three to eight different genes, we found that most embryos exhibited a unique phenotype, demonstrating successful injection of a single droplet per embryo (Fig. 1E and fig. S3, C and D). The frequency of each phenotype was close to the expected value, indicating proportionate representation of each droplet within a mixed pool. Finally, the injected DNA barcodes could be recovered at least up to 7 days post fertilization (dpf) (fig. S3E). Retrieval and sequencing of the barcode from the injected embryos revealed a high genotype-phenotype correlation. Although we used single-guide RNA DNA templates as the basis of the barcodes here, other barcoding strategies may be feasible (see the supplementary text).

Next, we tested whether MIC-Drop could identify genes responsible for a particular phenotype from a list of candidate genes (Fig. 2A). We spiked droplets targeting the *tyr* or *npas4l* genes into a larger pool of droplets containing scrambled gRNAs such that the *tyr* or *npas4l* MIC-drops each represented 2% of the total. Hundreds of embryos were injected with the intermixed droplets, and the frequency of *sandy* and *cloche* phenotypes among the injected embryos was assessed. We observed frequencies of 1.7 ± 0.8% and 2.2 ± 0.8% for the *sandy* and *cloche* phenotypes, respectively (Fig. 2A, inset), comparable to the theoretical expected frequency of 2%, indicating that MIC-Drop screens are sensitive and may be a useful platform for a variety of applications requiring identification of genotype-phenotype relationships in vertebrates on a large scale.

Identifying the protein targets of small molecules remains one of the major challenges in chemical biology and pharmacology (*18*, *19*). We hypothesized that MIC-Drop could be used to identify the targets of small molecules that result in complex behavioral phenotypes in the zebrafish. As proof of principle, we used optovin, a small-molecule agonist of the *trpa1b* channel that allows photoactivatable behavioral modifications in zebrafish (*20*). We spiked droplets targeting the *trpa1b* channel into a collection of droplets containing scrambled gRNAs in a 1:20 ratio (Fig. 2B). Droplet-injected embryos were arrayed into 96-well plates, treated with optovin, and exposed to violet light flashes while simultaneously recording embryo movement. Treatment of wild-type zebrafish embryos with optovin resulted in a light-dependent motor response (fig. S4, A to C, and movie S2). Embryos that showed reduced or no movement in the assay were isolated and their barcodes sequenced for genotype verification. We found

[1]Department of Pharmacology and Toxicology, University of Utah, Salt Lake City, UT, USA. [2]Department of Neurobiology and Molecular Medicine Program, University of Utah School of Medicine, Salt Lake City, UT, USA. [3]Department of Cardiovascular Medicine, Genetics and Network Medicine, Brigham and Women's Hospital and Harvard Medical School, Boston, MA, USA. [4]Cardiovascular Research Center, Massachusetts General Hospital and Harvard Medical School, Boston, MA, USA.
*Corresponding author. Email: randall.peterson@pharm.utah.edu
†Present address: Cellular and Molecular Biology, University of Wisconsin-Madison, Madison, WI, USA.

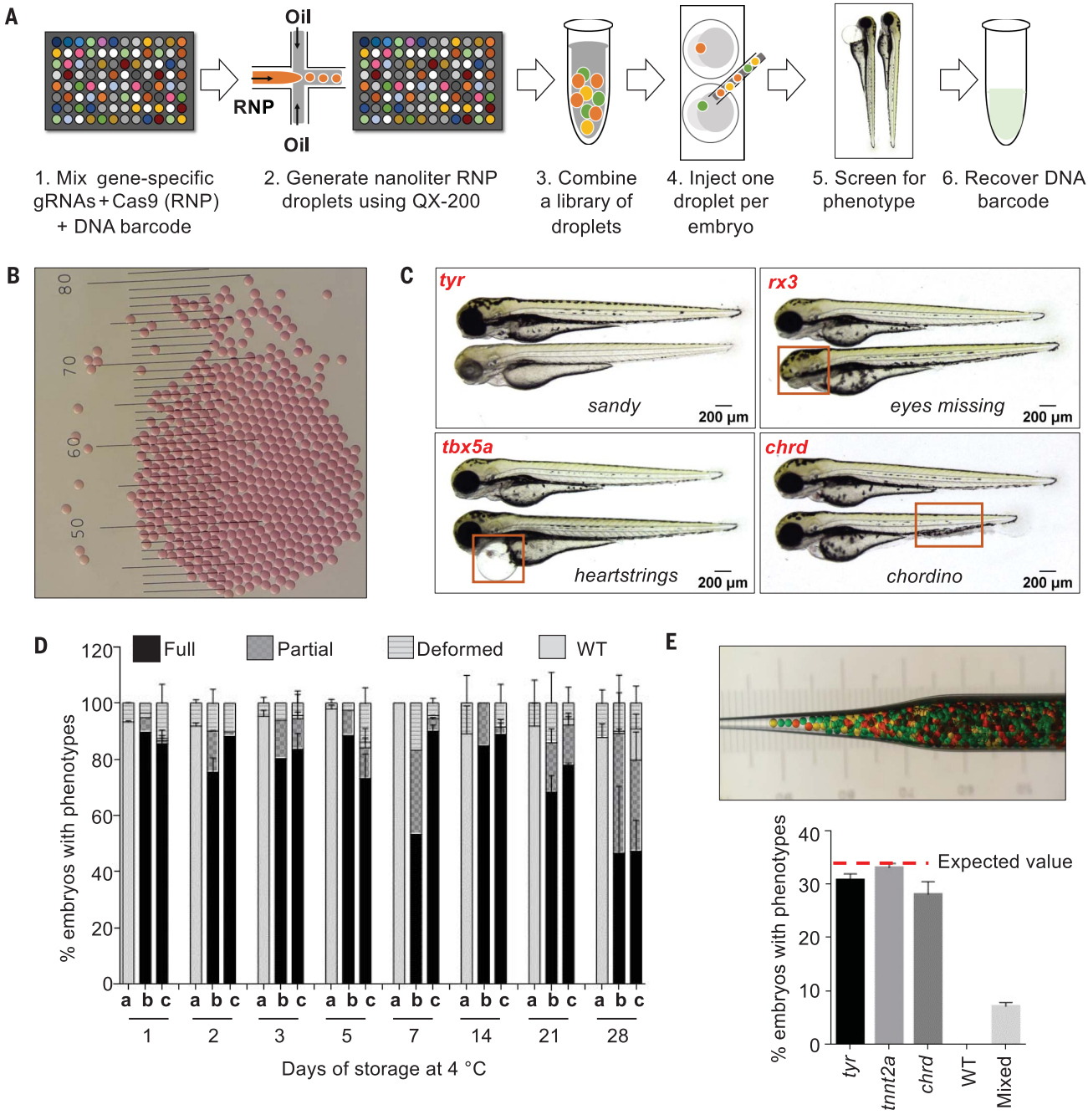

Fig. 1. MIC-Drop enables high-throughput CRISPR screens in zebrafish. (**A**) Workflow of the MIC-Drop platform. A microfluidics device generates nanoliter-sized droplets, each containing RNPs targeting a gene of interest and a unique DNA barcode associated with the gene. Droplets targeting multiple genes are intermixed, loaded into a single injection needle, and injected serially into one-cell zebrafish embryos. Embryos showing phenotypes of interest are isolated and the causative genotype is identified by retrieving and sequencing the barcode. (**B**) Droplets are uniform in size. Distance between bars is 0.1 mm. (**C**) Injection of droplets containing RNPs targeting *tyr*, *rx3*, *tbx5a*, and *chrd* genes recapitulates known mutant phenotypes in F_0, highlighted by red boxes. (**D**) RNP-containing droplets are nontoxic and stable for prolonged storage, retaining activity for at least 28 days of storage at 4°C. (a) Uninjected; (b) traditional RNP injection; and (c) MIC-Drop injection. Day 1: (a) N = 118, (b) N = 79, (c) N = 134; day 2: (a) N = 116, (b) N = 68, (c) N = 59; day 3: (a) N = 120, (b) N = 88, (c) N = 87; day 5: (a) N = 129, (b) N = 78, (c) N = 95; day 7: (a) N = 105, (b) N = 102, (c) N = 107; day 14: (a) N = 94, (b) N = 53, (c) N = 77; day 21: (a) N = 123, (b) N = 100, (c) N = 32; and day 28: (a) N = 114, (b) N = 100, (c) N = 94. (**E**) Single-needle injection of intermixed droplets targeting three different genes (*tyr*, *tnnt2a*, and *chrd*) and subsequent phenotyping showing even representation of each droplet, with most of the embryos exhibiting only one of the three expected phenotypes; none (0%) was wild type. N = 230 total sequenced from three separate injections. Inset: Hundreds of artificially colored droplets (used as proxies for droplets targeting different genes) do not fuse when transferred to an injection needle.

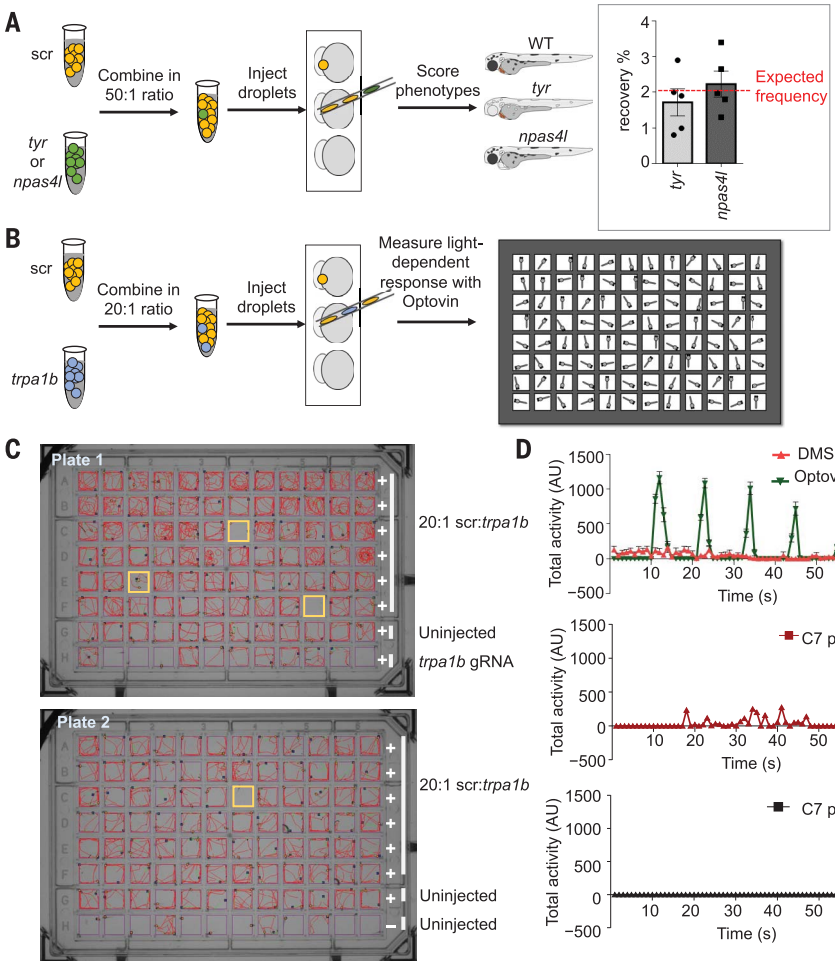

Fig. 2. MIC-Drop enables large-scale phenotypic screens and small-molecule target identification. (**A** and **B**) Schematic of a spike-in phenotypic (A) and behavioral (B) screen to test the robustness of the MIC-Drop platform. (A) For the phenotypic screen, droplets targeting either *tyr* or *npas4l* were intermixed with droplets containing nontargeting scrambled gRNAs (scr) in a 1:50 ratio. After single-needle droplet injection, the percentage of embryos showing *sandy* or *cloche* phenotypes was scored. Inset: The *sandy* and *cloche* phenotypes were recovered at a frequency of ~2%, which is the expected frequency from a 1:50 ratio mixture. (B) Similar to (A) except droplets targeting *trpa1b* were intermixed with scr droplets in a 1:20 ratio. After injection, embryos were arrayed in a multiwell plate, treated with optovin, and assayed for light-dependent motor response. (**C** and **D**) Tracking (C) and quantitation (D) of zebrafish movement showing that embryos injected with droplets targeting *trpa1b* are refractory to optovin- and light-induced motion response.

that 2 to 3% of embryos showed a complete loss of photoinduced motion (Fig. 2B and fig. S4D). Barcode sequencing revealed that 100% of the unresponsive embryos were of the *trpa1b* genotype. An additional ~2% of the embryos showed a photoinduced motor response despite being of the *trp1ab* genotype, likely because of incomplete loss of *trpa1b* function (fig. S4D). Thus, we were able to use the MIC-Drop platform to identify the target of optovin from among a library of nontarget candidates.

We envisioned that MIC-Drop could be used to rapidly perform large-scale, reverse genetic screens to uncover genes responsible for important phenotypes such as developmental defects in the cardiovascular system. Congenital heart disease is the most common form of birth defect in humans, affecting nearly 1% of all live births (*21*). Genetic factors play a strong causal role in the development of congenital heart disease, but a comprehensive understanding of all of the genes responsible is still lacking. We used publicly available RNA-sequencing datasets to curate a list of 188 poorly characterized genes that are enriched in the zebrafish embryonic heart tissue relative to skeletal muscle (Fig. 3, A and B; fig. S5, A and B; and tables S2 to S4) (*22*, *23*) and postulated that these genes might be important in vertebrate heart development. We generated a library containing MIC-Drops for all 188 genes plus several control genes (Fig. 3C and table S5). When two ohnologs of a gene were identified, two gRNAs for each ohnolog were combined in a single droplet. Morphological phenotyping of zebrafish embryos at 48 to 72 hours postfertilization after MIC-Drop injection identified 16 new genes, the loss of which resulted in a variety of specific cardiac or blood phenotypes (Fig. 3, D and E, and table S5). Secondary validation of these "hits" corroborated the findings of the initial screen, with 12 of 16 genes showing phenotypic penetrance in >20% of F_0 embryos (Fig. 3E). The screen identified gene mutations responsible for a range of phenotypes, including one mutation (*alad*) causing porphyria, two mutations (*gstm.3* and *atp6v1c1*) causing arrhythmia, and seven mutations (*actb2*, *clec19a*, *gse1*, *ppan*, *sf3b4*, *cox8a*, and *ddah2*) causing abnormal cardiac development, including defects in ventricular morphogenesis, cardiac looping, and formation of the atrioventricular valve and cardiac jelly.

Several reports have demonstrated that F_0 "crispant" phenotypes reliably reflect loss of target gene function, but nonspecific or off-target phenotypes are theoretically possible (see the supplementary text). To ensure that the phenotypes that we observed were caused by on-target gene knockout, we performed phenotype rescue with mRNA injection. *alad* crispants showed a complete loss of hemoglobin synthesis, which was rescued by injection of *alad* mRNA (Fig. 4A and fig. S6A), indicating a role for *alad* in erythropoiesis.

Voltage mapping of the *gstm.3* and *atp6v1c1* crispants showed slowed atrial and ventricular conductions and altered action potential duration (Fig. 4B and fig. S6B). We identified *atp6v1c1b* as the ohnolog responsible for the ventricular arrhythmia phenotype (fig. S6C). GSTM3 was recently identified as a risk factor in Brugada syndrome with increased susceptibility to sudden cardiac death (*24*). Germline *gstm.3* zebrafish mutants exhibited ventricular arrhythmia, corroborating our results observed in MIC-Drop crispants. Loss of function of several genes resulted in cardiac development defects. β-actin (*actb1* and *actb2*) crispants showed cardiac edema; a small, silent ventricle with

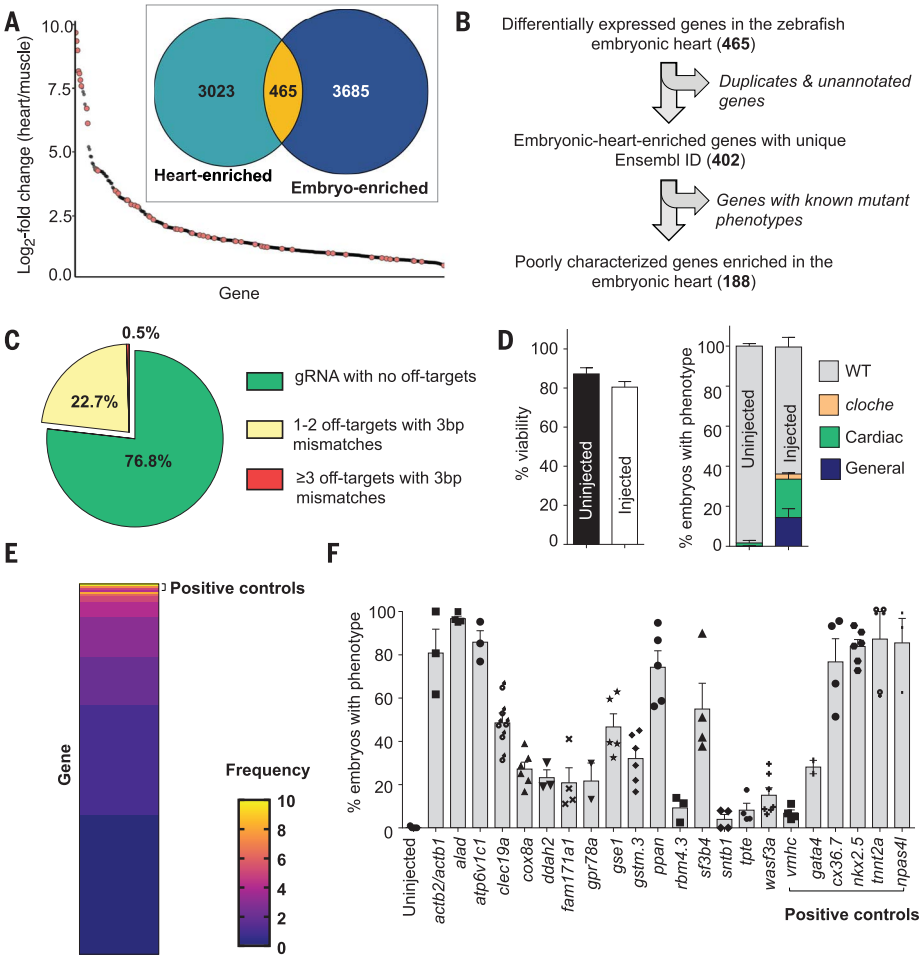

Fig. 3. A genetic screen to identify new regulators of cardiovascular development. (**A**) A publicly available dataset was used to populate a list of candidate genes enriched in the embryonic zebrafish heart. About 14% of the genes (orange dots) have reported cardiac phenotypes in ZFIN, suggesting enrichment of genes important in heart development. (**B**) Filtering to remove genes with known mutant phenotypes yielded 188 poorly characterized genes potentially important for cardiovascular development in zebrafish. (**C**) gRNA sequences with fewer off-targets were prioritized. (**D**) MIC-Drop screen of the 188 candidate genes and subsequent phenotyping showing no significant differences in viability between uninjected and droplet-injected embryos by 3 dpf. Left: uninjected, *N* = 1801, injected, *N* = 2502; right: uninjected, *N* = 1571, injected, *N* = 2013. Embryos with gross morphological defects at 3 dpf (~15%) were removed and the barcodes of those with cardiac defects were sequenced. Droplets targeting *npas4l* were spiked-in at a 2% proportion as a positive control. (**E**) Barcode sequencing of embryos displaying any cardiac phenotype (e.g., looping defect, chamber dysmorphogenesis, valve defect, arrhythmia, etc.) yields "hit" candidates. Heat map shows the observed frequency of each barcode. As positive controls, barcodes for *tnnt2a*, *nkx2.5*, and *npas4l* are enriched in the set of embryos exhibiting any visible cardiac phenotype. Genes with barcode frequency of ≥4 (binomial probability ≤ 0.05) or with consistent cardiac phenotypes were considered for secondary validation. (**F**) Secondary validation by direct RNP injection corroborated the screening results and identified 12 new genes, the loss of which resulted in cardiac phenotypes in at least 20% of F_0 embryos. WT, *N* = 238; *actb2/actb1*, *N* = 124; *alad*, *N* = 137; *atp6v1c1*, *N* = 135; *clec19a*, *N* = 182; *cox8a*, *N* = 130; *ddah2*, *N* = 126; *fam171a1*, *N* = 259; *gpr78a*, *N* = 186; *gse1*, *N* = 266; *gstm.3*, *N* = 199; *ppan*, *N* = 304; *rbm4.3*, *N* = 153; *sf3b4*, *N* = 307; *sntb1*, *N* = 107; *tpte*, *N* = 209; *wasf3a/b*, *N* = 130; *vmhc*, *N* = 107; *gata4*, *N* = 106; *cx36.7*, *N* = 147; *nkx2.5*, *N* = 186; *tnnt2a*, *N* = 124; and *npas4l*, *N* = 103.

reduced cardiomyocytes; leaky blood vessels; and gross craniofacial defects (Fig. 4C and movie S3). Loss of *actb2* alone was sufficient to recapitulate the cardiac phenotypes without the gross morphological defects, suggesting that *actb2* and *actb1* have nonoverlapping roles (Fig. 4C and fig. S6, D and E). *clec19a*, a c-type lectin protein with unknown functions, was found to be important for the normal development of cardiac jelly and the atrioventricular valve in 3 dpf zebrafish embryos (Fig. 4D and movie S4). Additionally, *cox8a*, a component of the mitochondrial electron transport chain, and *ddah2*, an arginine-metabolizing enzyme, were shown to be important for normal cardiac looping and ventricular morphogenesis (fig. S7A). Finally, three other genes with limited annotation of their functions were identified as being important in heart development. Loss of *ppan*, *gse1*, and *sf3b4* resulted in cardiac abnormalities along with other development defects such as malformed cartilage in the jaw and pharyngeal arches (*ppan*), bent trunk (*gse1* and *sf3b4*), and craniofacial defects (*sf3b4*) causing embryonic lethality (Fig. 4, E and F; fig. S7B; and movies S5 and S6). Phenotypes associated with *actb2*, *ppan*, and *sf3b4* MIC-Drops were also rescued by coinjection of *actb2*, *ppan*, and *sf3b4* mRNAs (Fig. 4F and figs. S6 and S7), suggesting that the phenotypes are caused by loss of function of the targeted genes. Therefore, MIC-Drop enabled a highly efficient reverse-genetic CRISPR screen in an intact vertebrate, leading to the discovery of several genes that contribute to diverse aspects of cardiac development or function.

In conclusion, we have developed a microfluidics-based platform for large-scale CRISPR screens in a vertebrate. CRISPR screens have previously been performed in cultured cells (*25*, *26*), but genome editing in vertebrates has primarily been done one gene at a time. The few small-scale CRISPR screens reported in vertebrates were enabled by brute force scaling of single-gene methods for generating, tracking, and analyzing individual genes, with little economy of scale (*10*, *11*, *27*). By intermixing droplets targeting many genes and incorporating a barcode for retrospective target identification, the MIC-Drop platform enables zebrafish to be injected, housed, and analyzed en masse, with rapid identification of the target genes in individuals exhibiting phenotypes of interest. The pilot screen reported here quickly discovered several genes important for cardiovascular development and function. This screen of 188 genes was completed efficiently by a single investigator and could readily be scaled to thousands of genes or even to full genome scale (see the supplementary text). Moreover, MIC-Drop is versatile and can conceivably be used, not just for gene knockout, but also for other screens such as CRISPR activation and inactivation screens, screens that mutate promoter or regulatory elements to create "transcript-less" mutants (*28*), and functional screens of noncoding genetic elements (see the supplementary text). Finally, the platform could be adapted for use in other model organisms, including *Xenopus* and mouse embryos, in which F_0 crispants

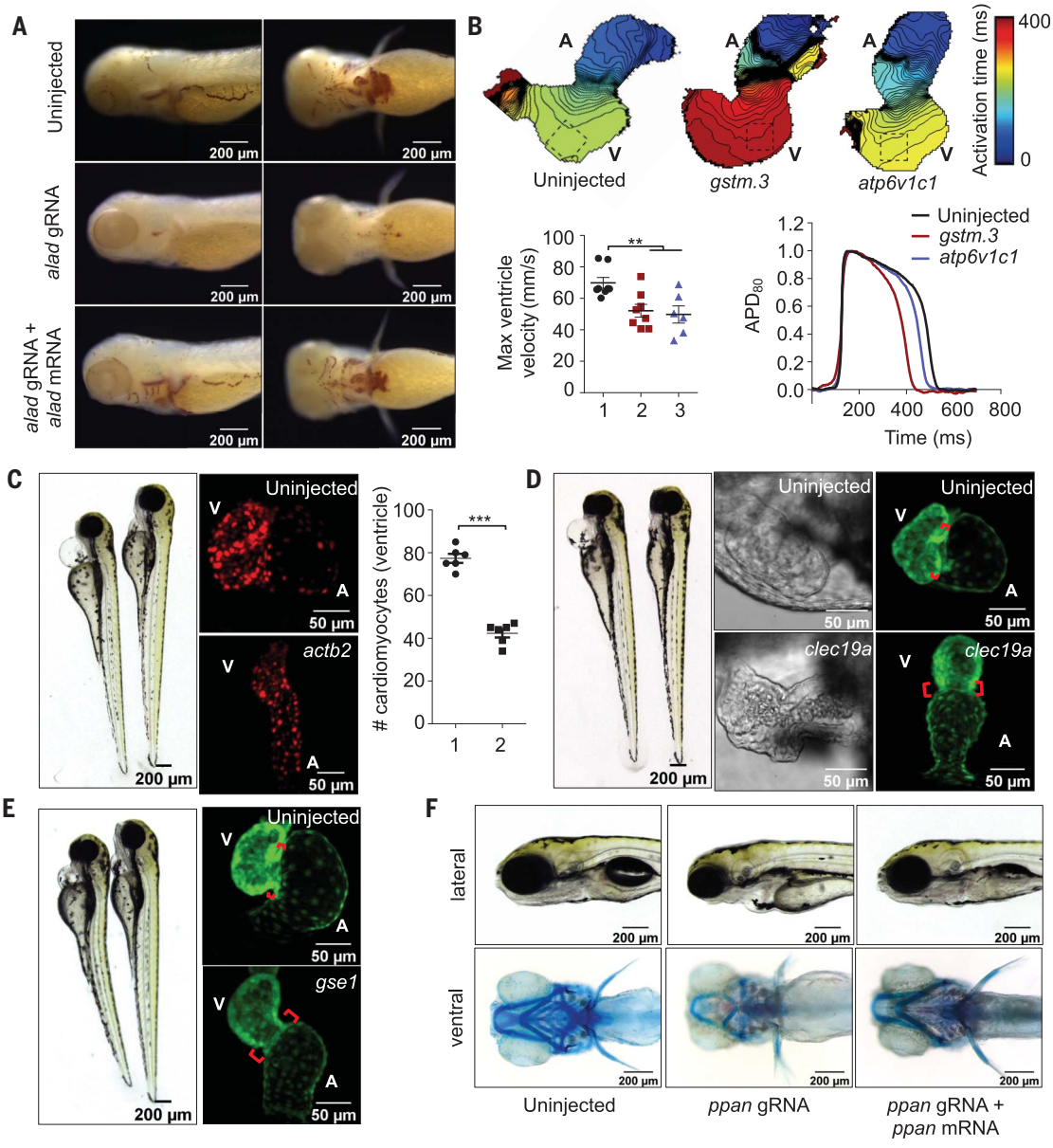

Fig. 4. CRISPR screen using MIC-Drop identifies new genes responsible for cardiovascular development. (**A**) *o*-dianisidine staining showing that loss of *alad* results in porphyria, which can be rescued by coinjection of *alad* mRNA. (**B**) Loss of *gstm.3* or *atp6v1c1* results in abnormal cardiac electrophysiology. Isochronal maps and action potential measurements reveal reduced conduction velocities and shorter ventricular action potential duration in the *gstm.3* and *atp6v1c1* crispants relative to uninjected controls. 1: Uninjected; 2: *gstm.3* crispants; 3: *atp6v1c1* crispants. Data are presented as mean ± SEM (**$P \leq 0.01$; ***$P \leq 0.001$). (**C** to **F**) Loss of *actb2* (C), *clec19a* (D), *gse1* (E), and *ppan* (F) result in distinct cardiac malformations. *actb2* crispants have a small ventricle with reduced number of ventricular cardiomyocytes. 1: Control; 2: *actb2*-targeting gRNAs (C). Loss of *clec19a* and *gse1* result in abnormal morphogenesis and an extended atrio-ventricular canal relative to wild-type embryos [(D) and (E)]. Alcian blue staining of *ppan* crispants showing abnormal jaw and skull development, which was rescued by *ppan* mRNA injection. The embryos also display cardiac edema and a silent ventricle (F).

are shown to recapitulate known germline mutant phenotypes (*29*, *30*), and likely also in other model organisms amenable to microinjection, such as sea urchins, fruit flies, and nematodes. Thus, the MIC-Drop platform enables in vivo vertebrate CRISPR experiments to be performed with the speed, efficiency, and scale previously available only to in vitro systems.

REFERENCES AND NOTES

1. E. E. Patton, L. I. Zon, *Nat. Rev. Genet.* **2**, 956–966 (2001).
2. A. Amsterdam *et al.*, *Proc. Natl. Acad. Sci. U.S.A.* **101**, 12792–12797 (2004).
3. W. Driever *et al.*, *Development* **123**, 37–46 (1996).
4. P. Haffter *et al.*, *Development* **123**, 1–36 (1996).
5. B. M. Weinstein *et al.*, *Development* **123**, 303–309 (1996).
6. M. Sison, J. Cawker, C. Buske, R. Gerlai, *Lab Anim. (NY)* **35**, 33–39 (2006).
7. R. A. Jain *et al.*, *Curr. Biol.* **28**, 1357–1369.e5 (2018).
8. W. Y. Hwang *et al.*, *Nat. Biotechnol.* **31**, 227–229 (2013).
9. M. Jinek *et al.*, *Science* **337**, 816–821 (2012).
10. W. Pei *et al.*, *NPJ Regen. Med.* **3**, 11 (2018).
11. G. K. Varshney *et al.*, *Genome Res.* **25**, 1030–1042 (2015).
12. F. Kroll *et al.*, *eLife* **10**, e59683 (2021).
13. A. N. Shah, C. F. Davey, A. C. Whitebirch, A. C. Miller, C. B. Moens, *Nat. Methods* **12**, 535–540 (2015).
14. K. Hoshijima *et al.*, *Dev. Cell* **51**, 645–657.e4 (2019).
15. J. A. Gagnon *et al.*, *PLOS ONE* **9**, e98186 (2014).
16. A. Burger *et al.*, *Development* **143**, 2025–2037 (2016).
17. R. S. Wu *et al.*, *Dev. Cell* **46**, 112–125.e4 (2018).
18. M. Jost, J. S. Weissman, *ACS Chem. Biol.* **13**, 366–375 (2018).
19. C. Fellmann, B. G. Gowen, P. C. Lin, J. A. Doudna, J. E. Corn, *Nat. Rev. Drug Discov.* **16**, 89–100 (2017).
20. D. Kokel *et al.*, *Nat. Chem. Biol.* **9**, 257–263 (2013).
21. S. Zaidi, M. Brueckner, *Circ. Res.* **120**, 923–940 (2017).
22. L. Wang, X. Ma, X. Xu, Y. Zhang, *Sci. Rep.* **7**, 1250 (2017).
23. Y. H. Shih *et al.*, *Circ. Cardiovasc. Genet.* **8**, 261–269 (2015).
24. J. J. Juang *et al.*, *EBioMedicine* **57**, 102843 (2020).
25. T. Wang, J. J. Wei, D. M. Sabatini, E. S. Lander, *Science* **343**, 80–84 (2014).
26. O. Shalem *et al.*, *Science* **343**, 84–87 (2014).
27. W. Tang *et al.*, *iScience* **23**, 100942 (2020).
28. M. A. El-Brolosy *et al.*, *Nature* **568**, 193–197 (2019).
29. I. L. Blitz, J. Biesinger, X. Xie, K. W. Y. Cho, *Genesis* **51**, 827–834 (2013).
30. H. Wang *et al.*, *Cell* **153**, 910–918 (2013).
31. C. Herdman, Code for: MIC-Drop: A platform for large-scale in vivo CRISPR screens, Version 1.0, Zenodo (2021). https://doi.org/10.5281/zenodo.5154537.

ACKNOWLEDGMENTS

We thank A. Serrano for assistance in imaging, B. Bisgrove for advice on phenotyping and for providing a list of candidate cardiac development genes, B. Demarest for advice on

RNA-sequencing data analysis, and members of the Peterson laboratory for their insights and critical feedback at all stages of the project. We also acknowledge the Centralized Zebrafish Animal Resource (CZAR) for providing zebrafish husbandry and microinjection equipment. **Funding:** This work was supported by the NIH (grant 5R01GM134069-02 to R.T.P. and J.J.Y., grant UM1 HL098160 to H.J.Y., NINDS grant U54-NS079201 to C.A.M., and OD grant R24OD017870 to C.A.M.) and by the American Heart Association (postdoctoral fellowship 827636 to S.P.).
Author contributions: S.P. and R.T.P contributed to conception and design, collection, analysis, and interpretation of the data, and manuscript writing. J.J.Y. contributed to conceptualization and experimental design. C.H. and H.J.Y. performed RNA-sequencing data analysis. M.B. and C.A.M. performed and interpreted cardiac voltage-mapping experiments. K.C. and Z.P.H. provided help with testing and optimizing the MIC-Drop platform. All authors contributed to the writing and review of the manuscript. **Competing interests:** S.P., J.J.Y., and R.T.P. have applied for a patent covering the technology described herein. R.T.P. has received honoraria (NIH) and expert testimony fees (Sterne Kessler/University of California) for work related to CRISPR technology. **Data and materials availability:** All data are available in the main text or the supplementary materials. All RNA-sequencing data are available on Gene Expression Omnibus under project accession no. GSE85416. Code for the analysis, including processed data, is available on Zenodo (*31*). Reagents will be made available upon request to the corresponding author.

SUPPLEMENTARY MATERIALS

science.sciencemag.org/content/373/6559/1146/suppl/DC1
Materials and Methods
Supplementary Text
Figs. S1 to S7
Reference (*32*)
MDAR Reproducibility Checklist
Tables S1 to S5
Movies S1 to S6

View/request a protocol for this paper from *Bio-protocol*.

7 April 2021; accepted 3 August 2021
10.1126/science.abi8870

Science

MIC-Drop: A platform for large-scale in vivo CRISPR screens

Saba ParvezChelsea HerdmanManu BeerensKorak ChakrabortiZachary P. HarmerJing-Ruey J. YehCalum A. MacRaeH. Joseph YostRandall T. Peterson

Science, 373 (6559), • DOI: 10.1126/science.abi8870

Screen time for CRISPR

CRISPR-Cas9 has been used to edit the genomes of organisms ranging from fruit flies to primates, but it has not been used in large-scale genetic screens in animals because generating, validating, and keeping track of large numbers of mutant animals is prohibitively laborious. Parvez *et al*. have developed Multiplexed Intermixed CRISPR Droplets, or MIC-Drop, a platform combining droplet microfluidics, en masse CRISPR injections, and barcoding, to enable large-scale genetic screens. In pilot phenotypic screens in zebrafish, MIC-Drop enabled rapid identification of the target of a small molecule and discovery of several new genes governing cardiovascular development. MIC-Drop is potentially scalable to thousands of targets and adaptable to diverse organisms and experiments. —DJ

Science (ISSN) is published by the American Association for the Advancement of Science. 1200 New York Avenue NW, Washington, DC 20005. The title *Science* is a registered trademark of AAAS.